II. MICROWAVE SPECTROSCOPY

Prof. M. W. Strandberg
Prof. R. L. Kyhl
Dr. J. M. Andrews, Jr.
S. N. Bromberg
G. Emo Capodilista
A. Fukumoto
M. C. Graham
R. Huibonhoa
J. G. Ingersoll
J. D. Kierstead
M. K. Maul
T. E. McEnally
R. M. Preer
S. Reznek
L. Rosen
W. J. Schwabe

A. OBSERVATIONS OF INCOHERENT PHONON PROPAGATION IN X-CUT QUARTZ

Using techniques similar to those of Gutfeld and Nethercot,[1] we have observed pulses of incoherent phonons propagating along the x axis of quartz. Figure II-1 is an oscilloscope picture of these pulses that have been generated in an aluminum film, approximately 100 Å thick, propagated along a rod of x-cut quartz, 3 mm in diameter and 19.3 mm long, and detected by means of a superconducting tin-alloy bolometer. The experiment was carried out at 3.6°K, where the maximum of the slope of the $\rho(T)$ function for the tin alloy occurred. The peak of the received signal is approximately 90 μv, corresponding to a bolometer current of 38 ma. The droop in the trailing edge of the signal at the right-hand side of the photograph is caused by the greatly decreased frequency response at 1 Mc and ringing in the video amplifier circuit. The lower trace in Fig. II-1 shows the generating pulse of ~40 watts peak power and 0.12 μsec in duration.

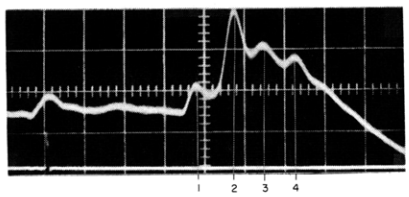

Fig. II-1. Pulses of incoherent phonons in x-cut quartz. Lower trace shows the generating pulse which marks zero on the time axis. The oscilloscope sweep rate is 1 μsec/cm.

The symmetry of the signal pulses indicates that the mechanism responsible for the broadening is not related to thermal time constants in either the generating or the receiving metallic films.

In a previous report,[2] we pointed out that the x axis of quartz is a pure-mode axis for the longitudinal and both of the transverse elastic modes and, furthermore, that the ultrasonic Poynting vectors should be collinear with the wave vectors along this axis for each of these three modes. Thus, each of these modes should be evident in a heat pulse directed along the x axis. In Fig. II-2, we show the three modes of coherent

phonons at 0.9 Gc, generated in the usual manner,[3] by means of a re-entrant microwave cavity.

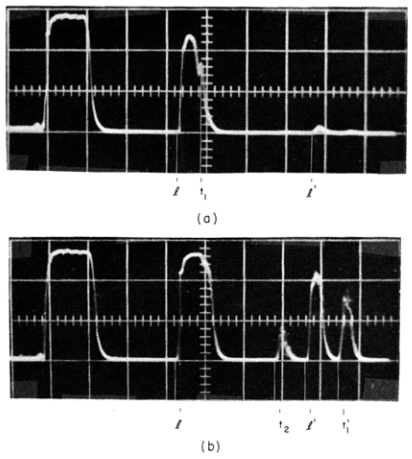

Fig. II-2.

(a) Coherent 0.9-Gc phonons in x-cut quartz. First pulse on the left is leakage from the transmitter and marks zero on the time axis.
(b) Same as (a) but with increased gain.

The oscilloscope sweep rate is 2 μsec/cm, but the pulses have made a round trip within the quartz rod and are received by the transmission cavity. Thus the scales of Fig. II-1 and II-2 can be considered the same for the purpose of total time-delay comparison. It was necessary to increase the path length in the 0.9-Gc coherent phonon experiment to resolve the longitudinal and fast-transverse modes.

In Fig. II-2a, ℓ denotes the leading edge of the first reflected longitudinal mode and t_1, the peak of the first reflected fast-transverse mode. The first reflected slow-transverse mode cannot be seen unless we increase the gain of the receiver. This is shown in Fig. II-2b, in which the peak of the slow-transverse mode is denoted t_2. Second reflections of these modes are denoted by primes in Fig. II-2. Note that, although the time scales and triggering are identical in Figs. II-2a and 2b, the leading edge of the longitudinal mode appears somewhat earlier in Fig. II-2b. This effect is caused by the finite rise time of the pulse. Thus comparisons between the leading edges of the longitudinal modes should be made between Fig. II-1 and Fig. II-2a, only.

Comparative measurements between the individual modes of the incoherent and the coherent phonon experiments are listed in Table II-1. We conclude that pulse no. 1 in the incoherent phonon experiment is actually a superposition of the longitudinal and fast-transverse pure modes. Pulse no. 4 corresponds most closely to the slow-transverse pure mode. Pulses X and Y are "extra" pulses, whose wave vectors are unknown, which happen to have Poynting vectors lying within the solid angle subtended by the receiving bolometer. In general, analytic determination of ultrasonic wave vectors as a function of the Poynting vector does not appear to be possible for an anisotropic propagation medium. Graphical methods are available,[4] and an approach by machine computation is under investigation.

At the present time, we can only speculate on the mechanism that is causing the heat pulse to broaden from 0.12 μsec to over 0.50 μsec for each of the pulses reaching the receiver. As we have pointed out in a previous report,[2] a resistive metallic film, bonded to a semi-infinite elastic medium and heated by means of a short pulse of electric energy,

Table II-1. Summary of pulse-delay data.

Experiment	Pulse	Reference	Delay (μsec)	Velocity (km/sec)	Mode
Incoherent Phonons (Fig. II-1)	1	leading edge	3.4	5.7	longitudinal
	1	peak	3.8	5.1	fast-transverse
	2	leading edge	4.3	4.5	X
	2	peak	4.7	4.1	X
	3	leading edge	5.2	3.7	Y
	3	peak	5.45	3.5	Y
	4	leading edge	6.0	3.2	slow-transverse
	4	peak	6.25	3.1	slow-transverse
Coherent Phonons at 0.9 Gc (Fig. II-2)	ℓ	leading edge	3.35*	5.8	longitudinal
	t_1	peak	3.8*	5.1	fast-transverse
	t_2	leading edge	5.9*	3.3	slow-transverse

*Since the coherent phonon experiment involved observations of reflected pulses, actual delay times have been divided by 2 in order to correspond to the single-pass measurements made on the incoherent phonon pulses.

is capable of generating simultaneously all of the vibrational modes of an elastic propagation medium that have their Poynting vectors lying within a solid angle of 2π about any point on the surface of the film. The degree of excitation of any given mode will depend upon the characteristic of the emission of the metallic generating film and on the phonon excitation spectrum of both the generating film and the elastic propagation medium. It seems likely that the characteristic of the emission of the generating film is essentially Lambertian, modified by the effects of the elastic mismatch between the metal and the propagation medium and by the detailed geometrical nature of the interface.

Thus each of the pulses in the incoherent phonon experiment (Fig. II-1) actually contains a mixture of all of the modes whose Poynting vectors lie within the solid angle subtended by the receiving bolometer. The arrival time of each mode depends not only upon the phase velocity of the mode but also upon the angle ψ between the wave vector $\vec{k}$ and the Poynting vector $\vec{S}$ and the angle σ between the Poynting vector $\vec{S}$ and the x axis of the quartz rod. These angles are illustrated in Fig. II-3 in which we have indicated a ray of elastic energy emanating from an arbitrary point O in the metallic generating film and propagating in the direction of the Poynting vector $\vec{S}$. The cross-hatching in the ray represents surfaces of constant phase, which are perpendicular to the wave vector $\vec{k}$. It must be emphasized that Fig. II-3 is a diagram presented for the sole purpose of defining angles. Physically, a single ray of incoherent elastic energy

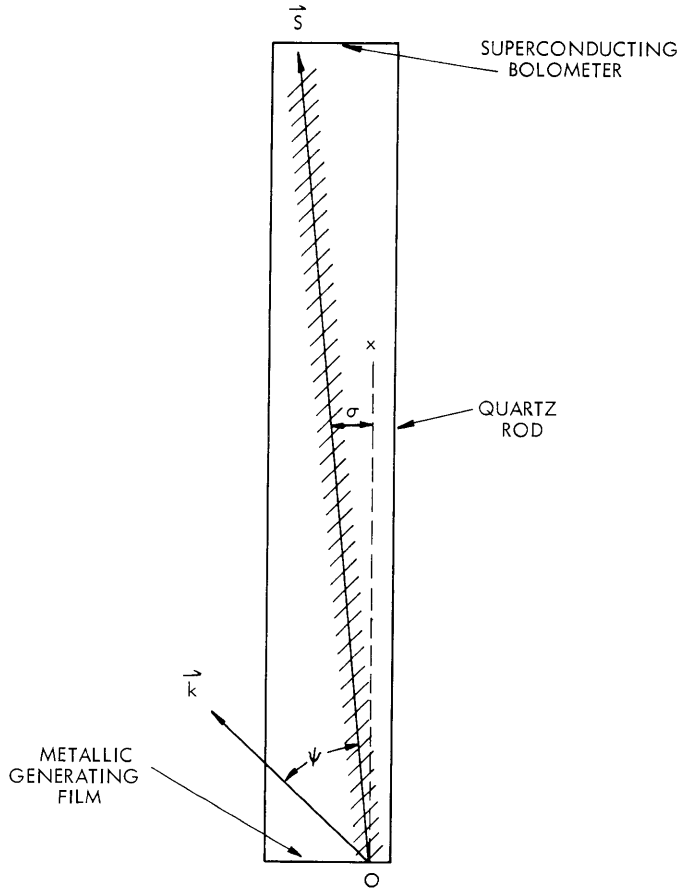

Fig. II-3. Phonon propagation in a rod of an anisotropic solid for arbitrary wave vector $\vec{k}$. The Poynting vector $\vec{S}$ denotes the direction of energy propagation.

cannot be characterized by a single wave vector, as there are no surfaces of constant phase. Rather, each ray contains an infinite distribution of $\vec{k}$ vectors, varying both in length and direction. It is just this sort of distribution in k-space that could give rise to the pulse broadening that is evident in Fig. II-1. In order to see this more clearly, we write an expression for the arrival time of elastic energy as a function of the wave vector $\vec{k}$ and the angles ψ and σ, which are also functions of the wave vector $\vec{k}$.

$$T_k = \frac{\ell \cos \psi}{v_k \cos \sigma} , \tag{1}$$

where T_k is the delay time of the k^{th} mode, v_k is the phase velocity of the k^{th} mode, $\psi = \psi(\vec{k})$ is the angle between wave vector $\vec{k}$ and Poynting vector $\vec{S}$, $\sigma = \sigma(\vec{k})$ is the angle between Poynting vector $\vec{S}$ and quartz rod axis, and ℓ is the length of the quartz rod. Thus the broadening of the incoherent pulses could arise from the distribution in the

arrival time T because the angle between the wave vectors $\vec{k}$ and the rod axis OX varies between zero and π, subject to the restriction $0 \leq \sigma \leq \sigma_{max}$. The maximum value of the angle σ is simply the angle subtended by the bolometer

$$\sigma_{max} = \tan^{-1}(d/\ell), \tag{2}$$

where d is the diameter of the quartz rod and ℓ is the length of the quartz rod.

The salient effect of the elastic mismatch between the metallic generating and receiving films and the quartz propagation medium manifests itself in the time constants of the generator and the detector. At low temperatures a thermal discontinuity, ΔT, exists at the interface between any two solid media in thermal contact whenever a heat flux passes across the interface. This so-called thermal boundary resistance, R_B^*, is similar to the Kapitza resistance between liquid helium and a solid and is defined as

$$\dot{Q} = \frac{A\Delta T}{R_B^*}, \tag{3}$$

where $\dot{Q}$ is the rate of heat flow (watts), A is the area of interface (cm^2), ΔT is the thermal discontinuity (°K), and R_B^* is the thermal boundary resistance (°K cm^2 $watts^{-1}$). A theoretical expression for the thermal boundary resistance has been derived by W. A. Little,[5] and is expressed as a function of the elastic properties of the adjoining media. Experimental values for the boundary resistance between indium and sapphire have been obtained by Neeper and Dillinger.[6] The results of their experiments compare favorably with an extrapolation of the theory of Little; hence, we have estimated the boundary resistance of a quartz-tin interface, using a similar extrapolation. Thus

$$R_B^* = 8T^{-3} \text{ °K cm}^2 \text{ watts}^{-1} \qquad \text{(estimated for quartz-tin).} \tag{4}$$

It is not entirely obvious that the Kapitza resistance between a liquid helium-metal interface should have the same order of magnitude as the thermal boundary resistance between quartz and tin; yet with gold and copper this has been the experimental observation[7]

$$R_K^* = 8T^{-3} \text{ °K cm}^2 \text{ watts}^{-1} \qquad \text{(observed for gold-liquid helium).} \tag{5}$$

We have no data on the Kapitza resistance of tin; we assume that the value for gold represents a very good approximation. The thermal time constant of a metallic film on a solid substrate submerged in liquid helium is determined by the parallel combination of the thermal boundary resistance and the Kapitza resistance.

$$\tau = \rho c_v d \frac{R_K^* R_B^*}{R_K^* + R_B^*} \text{ sec}, \tag{6}$$

where ρ is the density of the metallic film (gm cm^{-3}), c_v is the heat capacity of the metallic film (J gm^{-1} $°K^{-1}$), and d is the thickness of the metallic film (cm). Using recent data on the low-temperature heat capacity of tin, we find that the time constant of a 1000 Å film at 3.6°K is 10^{-9} sec. This figure supports our previous contention that the pulse broadening is not associated with the thermal response time of the bolometer.

In a subsequent experiment, a layer of glue, ~10^{-3} cm thick, was painted over the bolometer. Typical heat capacities of such materials are ten times greater than those for metals at helium temperature. We have no data on the thermal boundary and Kapitza resistances for glue, but perhaps it is relevant to point out that experimental values of these resistances vary less than an order of magnitude over a wide range of materials.[7] Assuming that the thermal resistances associated with the glue are not significantly different, we obtain a time constant, $\tau \sim 10^{-6}$ sec, for the glue-coated bolometer. Figure II-4 shows the pulses of incoherent phonons intercepted by the glue-coated bolometer. As expected, most of the mode structure has been lost.

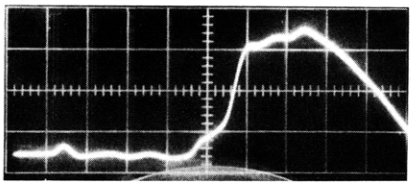

Fig. II-4. Incoherent phonons in x-cut quartz observed with a glue-coated bolometer.

Using an expression for the thermal discontinuity across an interface that is valid when the temperature difference is large compared with the ambient temperature,[5] we can estimate the temperature rise of our generating film.

$$\dot{Q} = \frac{A\left(T^4 - T_o^4\right)}{4R^* T^3}. \tag{7}$$

From VSWR measurements on the aluminum-generating film, we have determined that approximately 20 per cent of the input power is converted into heat in the film. Therefore, for a total power input of $\dot{Q} \approx 40$ watts, we find $T \sim 7°K$. (This is sufficiently high to call into question our tacit assumption of thermal equilibrium.) If we also assume that the frequency spectrum of the thermal vibration in our generating film can be characterized by a Planck distribution, we can estimate the order of magnitude of the dominant frequencies involved in the transport of thermal energy through the quartz rod:

$$\nu_{peak} \approx \frac{3kT}{h}. \tag{8}$$

The peak of the Planck distribution occurs at $\nu_{peak} \approx 0.4 \times 10^{12}$ sec^{-1} in our experiment. The lattice constant of quartz is approximately 5 Å. This places the edge of the first Brillouin zone at 6.3×10^{7} cm^{-1}. Thus, the maximum frequency that can be propagated on the longitudinal branch of the acoustic mode is given by

$$\nu_{max} = 5.7 \times 10^{12} \text{ sec}^{-1}. \tag{9}$$

For the slow-transverse branch,

$$\nu_{max} = 3.3 \times 10^{12} \text{ sec}^{-1}. \tag{10}$$

These considerations serve to point out a second possible origin of the signal-pulse broadening that is evident in Fig. II-1. From the foregoing analysis, it appears that a significant portion of the elastic energy of these incoherent phonon pulses is carried by modes whose frequencies are close to the cutoff frequency of the lattice. Whether dispersion effects are making an appreciable contribution to the pulse broadening is a subject for further investigation.

At low temperatures the mean-free path of a phonon in a crystal approaches the dimension of the crystal. Our observations are consistent with rectilinear propagation of the phonons, without evidence of the dominant scattering mechanism that characterizes heat flow in solids at room temperature. Thus we have observed the breakdown of the diffusion equation. As we have mentioned, approximately 20 per cent of our total input power is dissipated in the aluminum generating film. Of this, half flows directly to the liquid helium through the Kapitza resistance. Thus, for a peak input power of 40 watts, only ~4 watts enters the quartz rod through the thermal boundary resistance. Because of rectilinear propagation, only 4×10^{-3} watt intercepts the receiving bolometer directly, if we assume that the thermal energy at the generating film is distributed evenly over a solid angle of 2π.

In order to estimate the resulting voltage rise in the bolometer, we draw upon an expression for the responsivity of a bolometer.[8]

$$r = \frac{\Delta V}{\Delta \dot{Q}} = \frac{i\alpha R R^{*}}{2A}, \tag{11}$$

where ΔV is the voltage rise (volts), $\Delta \dot{Q}$ is the power input (watts), i is the bias current (amps), $\alpha = \frac{1}{R}\frac{dR}{dT}$ is the temperature coefficient of resistivity ($^{\circ}K^{-1}$), R is the resistance of the bolometer (ohms), R^{*} is the effective thermal resistance of bolometric film ($^{\circ}K$ cm^{2} watts^{-1}), and A is the area of the bolometric film (cm^{2}).

In Eq. 11 we have assumed that the bolometer is terminated in a load impedance

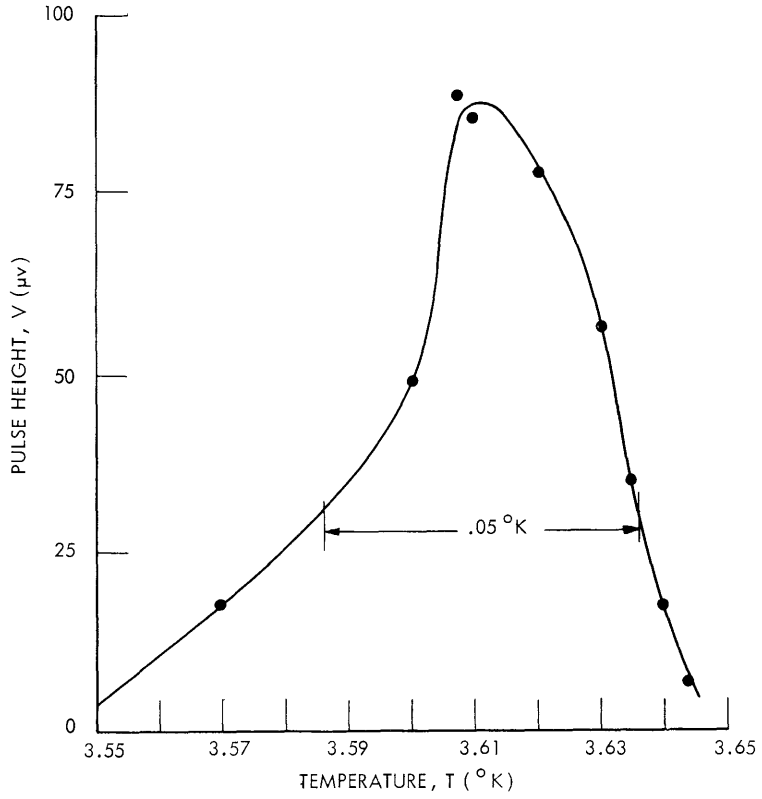

Fig. II-5. Signal voltage as a function of bolometer temperature. The peak occurs at the maximum slope of the resistivity for the superconducting transition of the bolometer.

equal to its own resistance, R. In order to estimate α, we plotted the received signal as a function of bolometer (ambient) temperature. This is shown in Fig. II-5. We see that the sensitive region of the bolometer occurs within a temperature range of 0.05°K. Since $\alpha \approx (\Delta T)^{-1}$, we estimate $\alpha \approx 20$. The resistance of the bolometer, R, is ~0.1 Ω, and the bias current was 38 ma for our observations. The effective thermal boundary resistance, previously calculated, is $\sim 4T^{-3}$, and the area, A, of the bolometer is 0.07 cm^2. These values, substituted in Eq. 11 yield a responsivity, r ~0.05 volts/watt. With 4×10^{-3} watt incident upon the bolometer, we expect a voltage rise of the order of 200 μv. Within the approximate nature of our calculation, this compares favorably with the observed voltage of 90 μv.

The author wishes to express appreciation to Professor J. F. Cochran, who pointed out the importance of the thermal-boundary resistance and the Kapitza resistance, and to acknowledge the assistance of Mr. M. C. Graham, who took part in the experiments.

J. M. Andrews, Jr.

1. R. J. von Gutfeld and A. H. Nethercot, Jr., Phys. Rev. Letters 12, 641 (1964).

2. J. M. Andrews, Jr., Incoherent phonon propagation in anisotropic media, Quarterly Progress Report No. 75, Research Laboratory of Electronics, M.I.T., October 15, 1964, pp. 5-7.

3. J. M. Andrews, Jr., Ultrasonic attenuation in superconductors, Quarterly Progress Report No. 70, Research Laboratory of Electronics, M.I.T., July 15, 1963, pp. 8-17.

4. M. J. P. Musgrave, Rept. Progr. Phys. 22, 74 (1959).

5. W. A. Little, Can. J. Phys. 37, 334 (1959).

6. D. A. Neeper and J. R. Dillinger, Phys. Rev. 135, A1028 (1964).

7. R. C. Johnson and W. A. Little, Phys. Rev. 130, 596 (1963).

8. R. A. Smith, F. E. Jones, and R. P. Chasmar, The Detection and Measurement of Infrared Radiation (Oxford University Press, London, 1957), p. 99.